

## Search for 8.4-keV Solar Axions Emitted in the $M1$ Transition in $^{169}\text{Tm}$ Nuclei

A. V. Derbin<sup>a</sup>, \* (ORCID: 0000-0002-4351-2255), I. S. Drachnev<sup>a</sup> (ORCID: 0000-0002-4064-8093),  
V. N. Muratova<sup>a</sup> (ORCID: 0000-0001-5532-7711), D. A. Semenov<sup>a</sup> (ORCID: 0009-0005-0286-0156),  
M. V. Trushin<sup>a</sup> (ORCID: 0000-0001-7620-0955), and E. V. Unzhakov<sup>a</sup> (ORCID: 0000-0003-2952-6412)

<sup>a</sup> Petersburg Nuclear Physics Institute, National Research Center Kurchatov Institute,  
Gatchina, Leningrad region, 188300 Russia

\*e-mail: derbin\_av@pnpi.nrcki.ru

Received June 28, 2023; revised June 29, 2023; accepted June 29, 2023

Axions with an energy of 8.4 keV emitted in the  $M1$  transition in  $^{169}\text{Tm}$  nuclei in the Sun are sought in the  $A + ^{169}\text{Tm} \rightarrow ^{169}\text{Tm}^* \rightarrow ^{169}\text{Tm} + (\gamma, e)$  (8.4 keV) reaction of resonant absorption by  $^{169}\text{Tm}$  nuclei on the Earth using a  $\text{Tm}_3\text{Al}_5\text{O}_{12}$  thulium garnet crystal as a bolometric detector. The flux of monochromatic 8.4-keV axions has been calculated. New constraints on the axion–nucleon coupling constants have been obtained and, as a result, new upper bounds on the axion mass  $m_A^{\text{KSVZ}} \leq 141$  eV and  $m_A^{\text{DFSZ}} \leq 244$  eV have been obtained at 90% C.L. in the KSVZ and DFSZ models, respectively.

DOI: 10.1134/S0021364023602026

### 1. INTRODUCTION

The probability of the production and detection of axions, i.e., hypothetical neutral pseudoscalar particles, which are introduced in the theory to explain the absence of the  $CP$  violation in strong interactions [1–3] and are well-justified candidates for the dark-matter constituents, is determined by the effective axion–photon ( $g_{A\gamma}$ ), axion–electron ( $g_{Ae}$ ), and axion–nucleon ( $g_{AN}$ ) coupling constants. The main reactions proposed to detect axions are the conversion of axions into photons in a magnetic or nuclear field, the decay of an axion into two photon, the Compton conversion, and the axioelectric effect.

In this work, we consider only the process of emission and absorption of axions in a nuclear magnetic transition occurring in the Sun and on the Earth, respectively. The sensitivity of the experiment is determined by the axion–nucleon coupling constants. Similar experiments were previously carried out with the  $^{57}\text{Fe}$  [4–6],  $^7\text{Li}$  [7–9], and  $^{83}\text{Kr}$  [10–12] nuclei.

After a series of experiments reliably excluded the “standard” model of the PQWW axion named after Peccei, Quinn, Weinberg, and Wilczek ([1–3], two classes of the models of the KSVZ (hadron axion) and DFSZ “invisible” axions called after Kim, Shifman, Vainshtein, and Zakharov [13, 14] and Dine, Fischler, Srednicki, and Zhitnitskii [15, 16], respectively, were proposed. The axion mass  $m_A$  and its decay constant  $f_A$  in both models are related to the respective charac-

teristics of the  $\pi^0$  meson as  $m_A f_A \approx m_\pi f_\pi (z^{1/2} / (1 + z))$ , where  $z = m_u/m_d$  is the ratio of the masses of the  $u$  and  $d$  quarks. The axion mass  $m_A$  is related to the decay constant  $f_A$  as [17, 18]

$$m_A = 5.69(5) \left( \frac{10^6 \text{ GeV}}{f_A} \right) \text{ eV}. \quad (1)$$

Constraints on the axion mass follow from experimental constraints on the coupling constants  $g_{A\gamma}$ ,  $g_{Ae}$ , and  $g_{AN}$ , which are model dependent.

Monochromatic axions should be emitted in magnetic transitions in  $^{57}\text{Fe}$  (14.4 keV) and  $^{83}\text{Kr}$  (9.4 keV) nuclei, where low-lying levels are excited due to a high temperature of 1.3 keV in the center of the Sun. The aim of this work is the search for the resonant absorption of monochromatic 8.4-keV axions, which are emitted in the  $M1$  transition in  $^{169}\text{Tm}$  nuclei, with the excitation of the first nuclear level of  $^{169}\text{Tm}$  nuclei. Gamma- and X-ray photons and conversion and Auger electrons, which are emitted upon the relaxation of the excited level, can be detected. The probability of the emission and subsequent absorption of axions depends only on the axion–nucleon coupling constant and is proportional to  $g_{AN}^4$ . This is the first search for 8.4-keV axions.

The search for solar axions with a continuous spectrum caused by the constants  $g_{A\gamma}$  (Primakoff axions)

and  $g_{Ae}$  (bremsstrahlung and Compton processes) using the  $^{169}\text{Tm}$  was proposed and performed in [19, 20].

The best known experiments are aimed at the search for solar axions produced through the conversion of thermal photons in the solar plasma field. Under the assumption of the axion–photon coupling, researchers attempt to detect axions through the inverse conversion in a laboratory magnetic field [21, 22] or in a crystal field [23, 24]. Photon count rates expected in these experiments are proportional to  $g_{A\gamma}^4$ . The theoretical and experimental works on the axion problem are reviewed in detail in [18].

## 2. FLUX OF 8.4-keV SOLAR AXIONS

The first excited level of the  $^{169}\text{Tm}$  nucleus has an energy of  $E_\gamma = 8.410$  keV and the spin and parity  $J^\pi = 3/2^+$ ; the admixture of the  $E2$  transition is 0.11% ( $\delta = 0.033$ ) [25]. The electron conversion coefficient is important for target–detector experiments, where conversion and Auger electrons are absorbed in the target. This coefficient for the transition under study is  $e/\gamma = 264$  ( $\eta = 3.79 \times 10^{-3}$ ) [25].

The solar axion flux depends on the energy  $E_\gamma$  and the lifetime  $\tau_\gamma$  of the level, the distribution of the abundance of the  $^{169}\text{Tm}$  isotope inside the Sun  $N(r)$ , the distribution of the temperature inside the Sun  $T(r)$ , and on the ratio of the probabilities of emission of axion and photon  $\omega_A/\omega_\gamma$  [4, 26]:

$$\Phi_A(r) = \frac{N}{\tau_\gamma} \frac{2 \exp(-E_\gamma/kT)}{(1 + 2 \exp(-E_\gamma/kT)) \omega_\gamma} \omega_A. \quad (2)$$

Due to the Doppler effect caused by the thermal motion of nuclei in the Sun, the spectrum of axions is a Gaussian with the standard deviation  $\sigma(T) = E_\gamma(kT(r)/M)^{1/2}$ , where  $M$  is the mass of the  $^{169}\text{Tm}$  nucleus. The total spectrum of axions is the sum of Gaussians with the standard deviations  $\sigma(T)$  determined by the temperatures at the points of emission of axions in the Sun.

The most intense flux of monochromatic axions from the Sun is due to the  $M1$  transition from the first excited level to the ground level of the  $^{57}\text{Fe}$  nucleus primarily because the abundance of iron in the Sun is high. The concentration of thulium is seven orders of magnitude lower, but the expected axion count rate increases due to a lower transition energy  $E_\gamma$ , a smaller Doppler broadening  $\sigma(T)$ , and the 100% abundance of the  $^{169}\text{Tm}$  isotope.

The fundamental difference of the  $M1$  transition in the  $^{169}\text{Tm}$  nucleus from similar transitions in the  $^{57}\text{Fe}$  and  $^{83}\text{Kr}$  nuclei is that it is mainly a proton transition. This is particularly important for the search for KSVZ

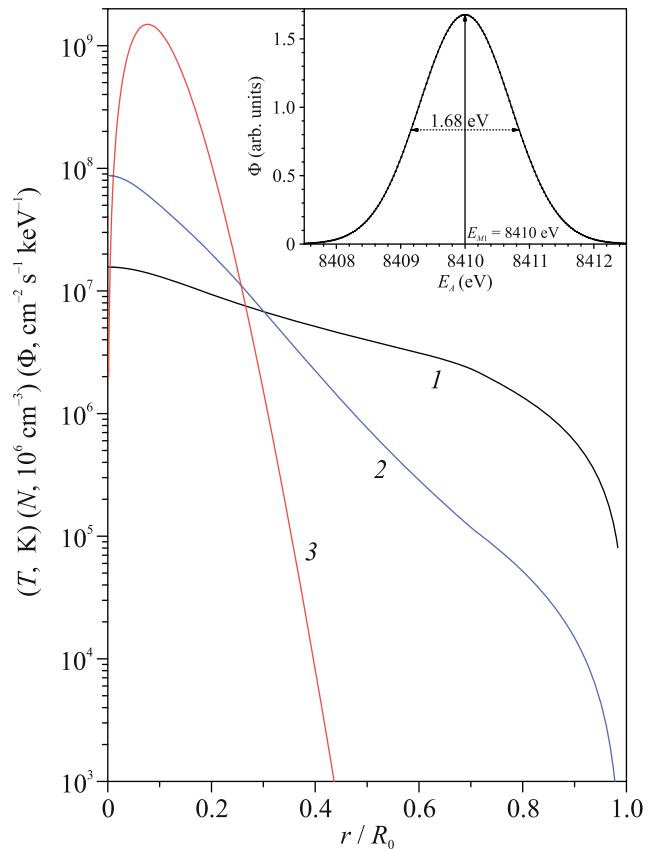


**Fig. 1.** Radial distributions of the (1) temperature  $T$  and (2) concentration  $N$  of  $^{169}\text{Tm}$  atoms and (3) the flux of axions  $\Phi$  from the  $r^2 dr$  layer for the parameters  $\omega_A/\omega_\gamma = 4 \times 10^{-14}$  and  $dr = 5 \times 10^{-3} R_\odot$ . The inset shows the energy spectrum of solar axions with an average energy of 8.41 keV.

axions whose coupling constant with the neutron is small. Furthermore, the ratio  $\omega_A/\omega_\gamma$ , which can vanish for neutron transitions, is nonzero for the proton transition.

We calculated the flux of axions for the standard solar model BS05 [27] with a high metallicity [28] as the sum of contributions from individual spherical layers each with the thickness  $dr$  and an individual temperature  $T$  and an individual thulium concentration  $N(r)$ . Figure 1 shows the dependence of the total axion flux from the  $r^2 dr$  layer on its radius  $r$ . It is seen that 90% of the total axion flux is emitted from the sphere with the radius  $r \leq 0.2R_\odot$ .

The differential spectrum is the sum of Gaussians each with the Doppler broadening  $\sigma(T)$ . The total energy spectrum of axions is presented in the inset of Fig. 1. It is well described by a Gaussian with the stan-

dard deviation  $\sigma = 0.78$  keV. The differential flux at the maximum of the distribution at  $E = 8.41$  keV is

$$\Phi(E) = 3.73 \times 10^{22} (\omega_A/\omega_\gamma) \text{ cm}^{-2} \text{ s}^{-1} \text{ keV}^{-1}. \quad (3)$$

The width of the resulting distribution is much larger than the energy of the recoil nucleus ( $2.2 \times 10^{-7}$  eV), the width of the nuclear level ( $\Gamma = 1.12 \times 10^{-7}$  eV), and the Doppler width of the level of  $^{169}\text{Tm}$  nuclei in the target ( $3.3 \times 10^{-3}$  eV) even at a temperature of  $T = 300$  K.

The ratio of the probabilities of axion and electromagnetic transitions  $\omega_A/\omega_\gamma$  was calculated in [29, 30]:

$$\frac{\omega_A}{\omega_\gamma} = \frac{1}{2\pi\alpha(1+\delta^2)} \left[ \frac{g_{AN}^0 \beta^* + g_{AN}^3}{(\mu_0 - 0.5)\beta^* + \mu_3 - \eta} \right]^2 \left( \frac{p_A}{p_\gamma} \right)^3, \quad (4)$$

where  $p_\gamma$  and  $p_A$  are the momenta of the photon and axion, respectively;  $\delta$  is the ratio of the probabilities of the  $E2$  and  $M1$  transitions;  $\mu_0 \approx 0.88$  and  $\mu_3 \approx 4.71$  are the isoscalar and isovector nuclear magnetic moments, respectively; and  $\beta^*$  and  $\eta$  are the parameters determined by particular nuclear magnetic elements. These parameter for the  $^{169}\text{Tm}$  nucleus with an odd number of nucleons and an unpaired proton can be estimated in the single-particle approximation as  $\beta^* = 1$  and  $\eta = 0.5$  [26].

The isoscalar  $g_{AN}^0$  and isovector  $g_{AN}^3$  parts of the axion–nucleon coupling constant, respectively, are model dependent. They can be expressed in terms of the effective axion–proton and axion–neutron coupling constants  $C_p$  and  $C_n$ , respectively [31, 32]:

$$\begin{aligned} g_{AN}^0 &= (M_N/2f_A)(C_p + C_n); \\ g_{AN}^3 &= (M_N/2f_A)(C_p - C_n), \end{aligned} \quad (5)$$

where  $M_N$  is the mass of the nucleon. The effective coupling constants  $C_p$  and  $C_n$  in turn depend on the axion–quark coupling constants [18, 31]. The calculations performed in [31] give the values  $C_p^{\text{KSVZ}} = -0.47(3)$  and  $C_n^{\text{KSVZ}} = 0.02(3)$  for the KSVZ model. As mentioned above, the axion–neutron coupling is strongly suppressed. The values  $C_p^{\text{DFSZ}} = -0.617 + 0.435 \sin^2 \beta \pm 0.025$  and  $C_n^{\text{DFSZ}} = 0.254 - 0.414 \sin^2 \beta \pm 0.025$  for the DFSZ axion depend on an additional parameter  $\beta$  [31]. We used the values  $C_p^{\text{DFSZ}} = 0.2712$  and  $C_n^{\text{DFSZ}} = 0.1248$  with the parameter  $\tan \beta = 10$ , which are found in [32]. Using Eq. (1), one can express the isoscalar and isovector constants  $g_{AN}^0$  and  $g_{AN}^3$  in terms of the axion mass  $m_A$ .

### 3. ABSORPTION RATE OF 8.4-keV AXIONS BY $^{169}\text{Tm}$ NUCLEI

The cross section  $\sigma(E_A)$  for the resonant absorption of axions with the energy  $E_A$  is given by the following expression similar to the cross section for the resonant absorption of  $\gamma$ -ray photons with the correction to the ratio  $\omega_A/\omega_\gamma$ :

$$\sigma(E_A) = 2\sqrt{\pi}\sigma_{0\gamma} \exp \left[ -\frac{4(E_A - E_{M1})^2}{\Gamma^2} \right] \left( \frac{\omega_A}{\omega_\gamma} \right), \quad (6)$$

where  $\sigma_{0\gamma} = 2.61 \times 10^{-19}$  cm<sup>2</sup> is the maximum cross section for the absorption of  $\gamma$ -ray photons by the  $^{169}\text{Tm}$  nucleus.

The total cross section for axion absorption can be obtained by integrating Eq. (6) for  $\sigma(E_A)$  over the spectrum of solar axions. The integration of the narrow distribution (6) over a wide spectrum of axions gives a value close to  $\Phi(E_{M1})$  in Eq. (3). The expected rate of resonant absorption of solar axions by the  $^{169}\text{Tm}$  nucleus is given by the expression

$$R_A = \pi\sigma_{0\gamma}\Gamma\Phi_A(E_{M1})(\omega_A/\omega_\gamma)^2 \quad (7)$$

and can be represented in the form

$$R_A = 3.35 \times 10^{-6} (\omega_A/\omega_\gamma)^2 \text{ s}^{-1}. \quad (8)$$

The ratio  $\omega_A/\omega_\gamma$  depends on the coupling constants  $g_{AN}^0$  and  $g_{AN}^3$  or  $C_p$  and  $C_n$ . As a result, the model-independent expression for the rate  $R_A$  of axion absorption by the  $^{169}\text{Tm}$  nucleus in units of inverse seconds per atom in terms of only the coupling constants has the form

$$R_A = 3.55 \times 10^{-6} (g_{AN}^0 + g_{AN}^3)^4 (p_A/p_\gamma)^6. \quad (9)$$

Substituting the expressions for the constants  $g_{AN}^0$  and  $g_{AN}^3$  in terms of the axion mass  $m_A$  obtained in the KSVZ and DFSZ models, one can express the rate of axion absorption by the  $^{169}\text{Tm}$  nucleus in terms of the axion mass measured in electronvolts:

$$\begin{aligned} R_A^{\text{KSVZ}} &= 4.88 \times 10^{-30} m_A^4 (p_A/p_\gamma)^6, \\ R_A^{\text{DFSZ}} &= 5.41 \times 10^{-31} m_A^4 (p_A/p_\gamma)^6. \end{aligned} \quad (10)$$

The total number of detected axions depends on the number of  $^{169}\text{Tm}$  nuclei in the target, measurement time, and detector efficiency. The probability of observing the 8.41-keV peak is determined by the background level of the experimental setup.

### 4. EXPERIMENTAL SETUP

To detect the resonant absorption of solar axions, we used a detector based on a cubic  $\text{Tm}_3\text{Al}_5\text{O}_{12}$  thulium garnet crystal with a side of 10 mm and a mass of 8.18 g including 4.97 g thulium, which was specially

grown at the Prokhorov General Physics Institute, Russian Academy of Sciences for our experiment and operated as a low-temperature bolometer [33].

The detector for measurements was placed in a vacuum cryostat at Max-Planck-Institut für Physik (Munich, Germany) and was cooled to a temperature of about 10 mK. The setup was placed on the ground and was calibrated using a standard calibrated  $^{55}\text{Fe}$  source. The energy resolution obtained for the 5.9-keV Mn  $K_{\alpha 12}$  line was  $\sigma = \text{FWHM}/2.35 = 0.4$  keV. Since the electron conversion coefficient  $e/\gamma$  is larger, the efficiency of detection of the 8.4-keV peak is  $\epsilon \approx 1.0$  with a high accuracy. The characteristics of the detector and experimental setup were described in detail in [33, 34].

As mentioned above, the relaxation of the excited level of the  $^{169}\text{Tm}$  nucleus is accompanied by the emission of conversion and Auger electrons, as well as X- and  $\gamma$ -ray photons. The  $^{169}\text{Tm}$  isotope enters the detector; consequently, the efficiency of the detection and resonant absorption is a factor of  $e/\gamma = 260$  higher than that in our previous target-detector experiments [19, 20].

## 5. RESULTS

The measurements were carried out for a live time of 3.86 days, and the resulting spectrum is shown in Fig. 3 in [34]. The background level near the 8.4-keV peak was 25 events per 0.1 keV per day. The measured spectrum is approximated in the range of 4.6–20 keV by the sum of a continuous background with four parameters, four Gaussians of the X-ray Mn  $K_{\alpha 1}$ ,  $K_{\alpha 2}$ , and  $K_{\beta}$  lines from the calibrated sources, and the expected 8.4-keV  $S_4$  axion peak whose position and width were matched to the parameters of the Mn  $K_{\alpha 1}$  line. The expected 8.4-keV axion peak was statistically insignificant.

To establish an upper bound on the number of counts in the peak, we used the standard method to determine the profile  $\chi^2(S_4)$  and the probability function  $P(\chi^2(S_4))$ . The upper bound on the number of peak events thus determined is  $S_{\text{lim}} = 128$  for 90% C.L. [34]. The determined upper bound on the number of events in the 8.41-keV peak provides bounds on the coupling constant  $C_p$  or  $(g_{AN}^0 + g_{AN}^3)$  and the axion mass  $m_A$  according to Eqs. (5), (9), and (10). The expected number of detected axions is

$$S_A = R_A N_{^{169}\text{Tm}} T \epsilon \leq S_{\text{lim}}, \quad (11)$$

where  $N_{^{169}\text{Tm}} = 1.77 \times 10^{22}$  is the number of  $^{169}\text{Tm}$  nuclei in the target,  $T = 3.34 \times 10^5$  s is the measurement time, and  $\epsilon = 1.0$  is the detection efficiency.

According to Eq. (9), under the condition  $(p_A/p_\gamma)^6 \approx 1$ , which is valid for the masses of the axion  $m_A < 2$  keV, we obtain the upper bound

$$|g_{AN}^0 + g_{AN}^3| \leq 8.89 \times 10^{-6}, \quad (12)$$

for 90% C.L. Bound (12) is a model-independent constraint on the coupling constants of the axion or any pseudoscalar axion-like particle to the nucleons. Using Eqs. (10), one can easily establish the following upper bound on the axion mass:  $m_A^{\text{KSVZ}} \leq 141$  eV and  $m_A^{\text{DFSZ}} \leq 244$  eV in the KSVZ and DFSZ-models, respectively.

The results should be compared to the upper bounds 0.145, 13.9, and 0.065 keV on the KSVZ axion mass obtained in experiments on the search for resonant absorption of solar axions by the  $^{57}\text{Fe}$  [4–6],  $^7\text{Li}$  [7–9], and  $^{83}\text{Kr}$  [10, 11] nuclei, respectively.

A more stringent astrophysical bound on the axion–proton coupling constant in the KSVZ model  $C_p^2 \leq (1-6) \times 10^{-17}$  follows from the measurement of the temperature of neutron stars in the presence of axion radiation [35–37].

## 6. CONCLUSIONS

The flux of monochromatic 8.41-keV solar axions, which are emitted upon the relaxation of the first nuclear level of  $^{169}\text{Tm}$  nuclei excited due to a high temperature in the Sun, has been calculated. The resonant absorption of these axions by  $^{169}\text{Tm}$  nuclei with the excitation of their first nuclear level has been sought. To detect particles emitted upon the relaxation of this level, a  $\text{Tm}_3\text{Al}_5\text{O}_{12}$  crystal has been used as a low-temperature bolometer. As a result, new upper bounds on the axion mass  $m_A^{\text{KSVZ}} \leq 141$  eV and  $m_A^{\text{DFSZ}} \leq 244$  eV have been obtained at 90% C.L. in the KSVZ and DFSZ models, respectively.

## FUNDING

This work was supported by the Russian Science Foundation, project no. 22-22-00017.

## CONFLICT OF INTEREST

The authors declare that they have no conflicts of interest.

## OPEN ACCESS

This article is licensed under a Creative Commons Attribution 4.0 International License, which permits use, sharing, adaptation, distribution and reproduction in any medium or format, as long as you give appropriate credit to the original author(s) and the source, provide a link to the Creative Commons license, and indicate if changes were made. The images or other third party material in this article are included in the

article's Creative Commons license, unless indicated otherwise in a credit line to the material. If material is not included in the article's Creative Commons license and your intended use is not permitted by statutory regulation or exceeds the permitted use, you will need to obtain permission directly from the copyright holder. To view a copy of this license, visit <http://creativecommons.org/licenses/by/4.0/>.

## REFERENCES

1. R. D. Peccei and H. R. Quinn, Phys. Rev. Lett. **38**, 1440 (1977).
2. S. Weinberg, Phys. Rev. Lett. **40**, 223 (1978).
3. F. Wilczek, Phys. Rev. Lett. **40**, 279 (1978).
4. S. Mariyama, Phys. Rev. Lett. **75**, 3222 (1995).
5. A. V. Derbin, A. I. Egorov, I. A. Mitropol'sky, V. N. Muratova, D. A. Semenov, and E. V. Unzhakov, Eur. Phys. J. C **62**, 755 (2009).
6. A. V. Derbin, V. N. Muratova, D. A. Semenov, and E. V. Unzhakov, Phys. At. Nucl. **74**, 596 (2011).
7. M. Krčmar, Z. Krečák, A. Ljubičić, M. Stipčević, and D. A. Bradley, Phys. Rev. D **64**, 115016 (2001).
8. A. V. Derbin, A. I. Egorov, I. A. Mitropol'skii, and V. N. Muratova, JETP Lett. **81**, 365 (2005).
9. P. Belli, R. Bernabei, R. Cerulli, et al., Nucl. Phys. A **806**, 388 (2008).
10. Yu. M. Gavril'yuk, A. N. Gangapshev, A. V. Derbin, I. S. Drachnev, V. V. Kazalov, V. V. Kobychev, V. V. Kuz'minov, V. N. Muratova, S. I. Panasenkov, S. S. Ratkevich, D. A. Semenov, D. A. Tekueva, E. V. Unzhakov, and S. P. Yakimenko, JETP Lett. **101**, 664 (2015).
11. A. V. Derbin, I. S. Drachnev, A. M. Gangapshev, Yu. M. Gavril'yuk, V. V. Kazalov, V. V. Kobychev, V. V. Kuzminov, V. N. Muratova, S. I. Panashenko, S. S. Ratkevich, D. A. Tekueva, E. V. Unzhakov, and S. P. Yakimenko, J. Phys.: Conf. Ser. **934**, 012018 (2017).
12. Yu. M. Gavril'yuk, A. N. Gangapshev, A. V. Derbin, I. S. Drachnev, V. V. Kazalov, V. V. Kuzminov, M. S. Mikulich, V. N. Muratova, D. A. Tekueva, E. V. Unzhakov, and S. P. Yakimenko, JETP Lett. **116**, 13 (2022).
13. J. E. Kim, Phys. Rev. Lett. **43**, 103 (1979).
14. M. Shifman, A. Vainshtein, and V. Zakharov, Nucl. Phys. B **166**, 493 (1980).
15. M. Dine, W. Fischler, and M. Srednicki, Phys. Lett. B **104**, 199 (1981).
16. A. Zhitnitskii, Sov. J. Nucl. Phys. **31**, 2 (1980).
17. M. Gorgetto and G. Villadoro, J. High Energy Phys., No. 03, 033 (2019).
18. R. L. Workman, V. D. Burkert, V. Crede, et al. (Particle Data Group), Prog. Theor. Exp. Phys. **2022**, 083C01 (2022); 2023 update.
19. A. V. Derbin, S. V. Bakhlanov, A. I. Egorov, I. A. Mitropol'sky, V. N. Muratova, D. A. Semenov, and E. V. Unzhakov, Phys. Lett. B **678**, 181 (2009).
20. A. V. Derbin, A. S. Kayunov, V. N. Muratova, D. A. Semenov, and E. V. Unzhakov, Phys. Rev. D **83**, 023505 (2011).
21. P. Sikivie, Phys. Rev. Lett. **51**, 1415 (1983).
22. V. Anastassopoulos, S. Aune, K. Barth, et al., Nat. Phys. **13**, 584 (2017).
23. F. T. Avignone, D. Abriola, R. L. Brodzinski et al. (The SOLAX Collab.), Nucl. Phys. Proc. Suppl. **72**, 176 (1999).
24. E. Armengaud, Q. Arnaud, C. Augier, et al. (EDELWEISS Collab.), J. Cosmol. Astropart. Phys. **1311**, 067 (2013).
25. C. M. Baglin, Nucl. Data Sheets **109**, 2033 (2008).
26. W. C. Haxton and K. Y. Lee, Phys. Rev. Lett. **66**, 2557 (1991).
27. J. N. Bahcall, A. M. Serenelli, and S. Basu, Astrophys. J. **621**, L85 (2005).
28. N. Grevesse and A. J. Sauval, Space Sci. Rev. **85**, 161 (1998).
29. T. W. Donnelly, S. J. Freedman, R. S. Lytel, R. D. Peccei, and M. Schwartz, Phys. Rev. D **18**, 1607 (1978).
30. F. T. Avignone, C. Baktash, W. C. Barker, F. P. Calaprice, R. W. Dunford, W. C. Haxton, D. Kahana, R. T. Kouzes, H. S. Miley, and D. M. Moltz, Phys. Rev. D **37**, 618 (1988).
31. G. G. di Cortona, E. Hardy, J. P. Vega, and G. Villadoro, J. High Energy Phys., No. 01, 034 (2016).
32. F. T. Avignone III, R. J. Creswick, J. D. Vergados, P. Pirinen, P. C. Srivastava, and J. Suhonen, J. Cosmol. Astropart. Phys., No. 01, 021 (2018).
33. E. Bertoldo, A. V. Derbin, I. S. Drachnev, et al., Nucl. Instrum. Methods Phys. Res., Sect. A **949**, 162924 (2020).
34. A. H. Abdelhameed, S. V. Bakhlanov, P. Bauer, et al., Eur. Phys. J. C **80**, 376 (2020).
35. J. Keller and A. Sedrakian, Nucl. Phys. A **897**, 62 (2013).
36. A. Sedrakian, Phys. Rev. D **93**, 065044 (2016).
37. K. Hamaguchi, N. Nagata, K. Yanagi, and J. Zheng, Phys. Rev. D **98**, 103015 (2018).

*Translated by R. Tyapaev*